

NUMERICAL MODELLING OF DAMAGE ACCUMULATION IN CORTICAL BONE TISSUE

Martina Lovrenić-Jugović, Zdenko Tonković, Ivica Skozrit

Original scientific paper

This paper describes the numerical implementation and validation of a constitutive model for simulating the mechanical behaviour of human cortical bone tissue. The model incorporates linear viscoelasticity coupled with damage to predict the creep and creep-recovery responses, respectively. The material parameters are determined by fitting the experimental results reported in the published literature. A computational algorithm for the integration of the proposed constitutive model at the material point level is derived. The derived algorithm in conjunction with the tangent stiffness matrix is implemented in the finite element code ABAQUS. The model predictions are found to be in good agreement with the experimental data presented in literature.

Keywords: cortical bone, creep, damage, finite element modelling, recovery, viscoelasticity

Numeričko modeliranje akumuliranja oštećenja u kortikalnom koštanom tkivu

Izvorni znanstveni članak

U radu je opisana numerička implementacija i validacija konstitutivnog modela za simuliranje mehaničkog ponašanja ljudskog kortikalnog koštanog tkiva. Model spreže viskoelastičnost s oštećenjem za simulaciju puzanja i puzanja s naknadnim rasterećenjem. Parametri materijala određeni su aproksimacijom eksperimentalnih rezultata iz literature. Izveden je računalni algoritam za integriranje predloženog konstitutivnog modela na razini materijalne točke. Izvedeni algoritam zajedno s tangentnom matricom krutosti implementiran je u program ABAQUS koji se temelji na metodi konačnih elemenata. Dobiveno je dobro poklapanje rezultata računalne simulacije i eksperimentalnih podataka iz literature.

Ključne riječi: kortikalna kost, modeliranje konačnim elementima, oštećenje, puzanje, rasterećenje, viskoelastičnost

1

Introduction

Skeletal fragility has received considerable attention because of personal and financial challenges associated with the increased risk of fracture. Consequently, a special interest of research scientists has been directed to a better description of bone behaviour, both under normal and pathological conditions. Human cancellous bone, as well as cortical, is a complex anisotropic material. Experimental studies have presented the non-linear viscous behaviour of bone material [1, 2]. In addition, due to mechanical loads the bone displays internal adaptive remodelling, which is sensitive to the local strain rates, strain distributions, dynamic nature of the loads and to the number of loading cycles. As presented in [3], remodelling is regulated by the mineral metabolism and the appearance of microcracks. Though significant research has been undertaken, these remodelling mechanisms remain not fully understood.

In recent years, investigations into the damage behaviour of both cortical and cancellous bone have aroused a great interest. Damage accumulation is a critical component of the fracture process in bone under monotonic, creep and fatigue load conditions. Previous studies have reported that damage accumulation leads to the degradation of the mechanical properties of bone, such as stiffness, strength, toughness, and viscous response [4]. In addition, bone damage has been implicated as a cause of increased fragility and is believed that it initiates bone remodelling. Fatigue-induced microdamage is repaired by bone remodelling, but if damage accumulates too quickly, or if remodelling is deficient, fatigue failure may result. Hence, in the long term, damage could lead to increased knowledge about the stability of prosthetic implants, debilitating bone diseases, such as osteoporosis, and it could help reveal the mechanisms behind stress fractures, which are significant orthopedic concerns today. One of the key issues that has not been resolved is how and where this damage initiates in

bone microstructure.

Numerous attempts have been made to simulate and predict the viscous damage behaviour of bone in a computer model, combining the continuum mechanics theories with the finite element (FE) analysis, but the obtained solutions still have some shortcomings [5, 6]. Constitutive models, which have to represent the bone behaviour realistically, form the core of a finite element formulation. The presented research is motivated by the experimental data reported by Melnis et al. [1] and Parsamian [7] for the nonlinear time-dependent response of human cortical bone. Melnis et al. [1] investigated the uniaxial tensile creep behaviour of human cortical bone and demonstrated the development of nonlinear strains during loading and their recovery behaviour after unloading. In an experimental study by Parsamian [7] it is found that human cortical bone behaves as a linear viscoelastic material during tensile creep for stress levels below some threshold value of stress. Beyond this value, it behaves as a viscoelastic damage material [1, 2]. An algorithm which enables numerical modelling of viscoelastic/damage behaviour of cortical bone is proposed by Lovrenić-Jugović et al. in [8, 9]. The present paper is a continuation of that study where the viscoelastic deformation associated with creep and creep-damage is analyzed in detail for more accurate predictions. The objective of this study is to develop a new constitutive model for the cortical bone tissue that predicts the experimental viscoelastic damage behaviour in creep-recovery tests. The derived model is based on the ideas and approaches from Abdel-Tawab and Weitsman [10] and [11], developed for the swirl-mat composites. level is implemented into the finite element code The bone behaviour is modelled by using the theory of viscoelasticity and non-linear effects within the theory of continuum damage mechanics based on the thermodynamics of irreversible processes [12, 13]. The derived algorithm for the integration of the proposed three-dimensional constitutive model at the material point ABAQUS/Standard

[14]. The accuracy of the computational procedure is tested by comparing the computed results with the real experimental [1, 7] and numerical [15] data. Thereby, the creep-recovery deformation processes in cortical bone at different loading levels are considered.

The paper is organized as follows. Section 2 describes the viscoelastic/damage constitutive model developed within the framework of irreversible thermodynamics with internal state variables. The material parameters of the constitutive model determined by fitting experimental results from literature are presented in Section 3. In Section 4, the proposed computational algorithm for the integration of the constitutive model is shown. The numerical results are presented and discussed in Section 5. Finally, the conclusions are presented in Section 6.

2 Constitutive model

In previous studies, it has been found that cortical bone behaviour under tensile creep loading is characterized by three crucial regimes. The first regime is linear viscoelasticity for stress levels below some threshold value of stress. Beyond this value, the second and/or third regimes, which correspond to the damage and viscoplasticity modes, start. The second damage mode represents the generation and opening of microcracks leading to a stiffness (modulus) reduction and permanent strains. The third viscoplastic mode is due to friction of the closing (or sliding) of microcracks leading to permanent strains but no extension of damage [5, 6].

A schematic representation of the stress history and strain response of cortical bone during the creep and recovery period is presented in Fig. 1. As can be seen, upon the removal of the applied load, the viscoelastic strain ϵ_{VE} is recovered, while the viscoplastic strain ϵ_{VP} is permanent. In the constitutive model presented here, assuming small strains, the total strain $\epsilon(t)$ is decomposed into time-dependent viscoelastic, non-linear damage and viscoplastic components. For simplification purposes, the influence of permanent viscoplastic deformations is neglected without a significant loss in accuracy (e.g. see [7, 16]). Constitutive equations, originally developed by Abdel-Tawab, Weitsman, Smith and Schapery [10, 11, 17, 18] for engineering materials, are employed here to model the human cortical bone response.

2.1 Anisotropic three-dimensional behaviour

A constitutive model based upon the fundamental principles of irreversible thermodynamics and continuum mechanics is proposed in [10, 11] to account for the viscoelastic material response coupled with continuously distributed damage. According to this constitutive model, the viscoelastic strain-stress response assuming isothermal conditions is defined by the relation

$$\epsilon_{ij}(t) = \int_0^t J_{ijkl}(t-\tau) \frac{\partial \tilde{\sigma}_{kl}}{\partial \tau} d\tau, \tag{1}$$

where $J_{ijkl}(t)$ denotes the viscoelastic compliance tensor of the undamaged (virgin) material, while t and τ stand for time and retardation time, respectively. In this formulation, the

viscoelastic properties of the material are not functions of damage. It is assumed that the time-dependent stress and damage influence the viscoelastic strain through the time-dependent effective stress, $\tilde{\sigma}_{kl}$ [12, 13]. Generally, in the case of three-dimensional deformations and damage, the effective stress tensor $\tilde{\sigma}_{kl}$ is given by the following transformation

$$\tilde{\sigma}_{ij} = M_{ijkl} \sigma_{kl}, \tag{2}$$

where M_{ijkl} is the damage effective tensor that characterizes the state of damage and σ_{kl} is the Cauchy stress tensor. The damage effective tensor M_{ijkl} is a fourth rank valued function of the damage w_{mnop} such that [10-13] when

$$w_{mnop} = 0 \rightarrow M_{ijkl} = I_{ijkl} = \frac{1}{2}(\delta_{ik} \delta_{jl} + \delta_{il} \delta_{jk}), \tag{3}$$

where I_{ijkl} is the identity tensor and δ_{ij} represents the Kronecker delta, respectively. Throughout this paper, the standard summation convention on repeated indices is used.

As presented in [10, 11], the viscoelastic compliance tensor $J_{ijkl}(t)$ can be decomposed into instantaneous (elastic) J_{ijkl}^0 and transient (time-dependent) $\Delta J_{ijkl}(t)$ parts of the undamaged material as

$$J_{ijkl} = J_{ijkl}^0 + \Delta J_{ijkl}(t), \tag{4}$$

where

$$J_{ijkl}^0 = J_{ijkl}^e - \sum_n \Delta J_{ijkl}^n, \tag{5}$$

$$\Delta J_{ijkl}(t) = \sum_n \Delta J_{ijkl}^n (1 - e^{-t/\tau_n}). \tag{6}$$

In Eqs (5) and (6) J_{ijkl}^e represents the initial compliance tensor. For the case of isotropic damage mechanics, the damage variable w_{mnop} is the single scalar variable and the damage evolution equations are as follows

$$w_{mnop} = w I_{mnop}, \tag{7}$$

$$M_{mnop} = \frac{1}{1-w} I_{mnop}. \tag{8}$$

2.2 Uniaxial creep model

The above three-dimensional continuum damage mechanics constitutive model is utilized to predict the time-dependent response of cortical bone tissue. The primary aim of the research is to simulate the creep-damage behaviour of that material. A relatively limited number of experimental studies describe the cortical bone response under uniaxial creep loading. Considering a one-dimensional case, the total viscoelastic strain coupled with damage, defined by Eq. (1), takes the following form

$$\epsilon_{11}(t) = \int_0^t J_{1111}(t-\tau) \frac{d\tilde{\sigma}_{11}}{d\tau} d\tau, \tag{9}$$

or

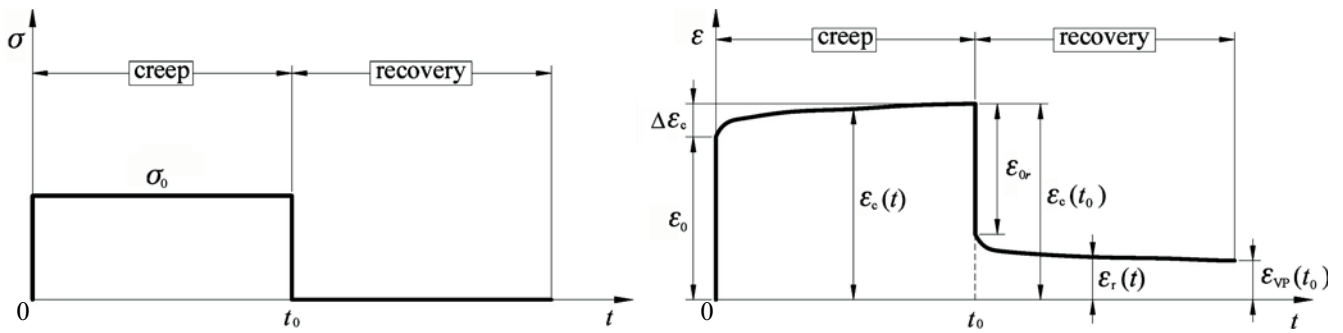


Figure 1 Schematic representation of the stress history and strain response during the creep-recovery period

$$\varepsilon_{11}(t) = \int_0^t \left[J_{ijkl}^0 + \Delta J_{ijkl}(t)(t-\tau) \right] \frac{d\tilde{\sigma}_{11}}{d\tau} d\tau \quad (10)$$

Using Eq. (2) and by means of Eqs (3), (7) i (8), the effective stress may be expressed in the standard form

$$\tilde{\sigma} = \frac{\sigma}{1-w(t)}, \quad (11)$$

where $w(t)$ is the scalar damage variable associated with continuously distributed microcracks ($0 < w < 1$). According to Pipkin [19], the following expression for the transient part of the compliance tensor (Eq. (6)) is adopted

$$\Delta J_{1111}(t) = \sum_n \Delta J_{1111}^n (1 - e^{-t/\tau_n}) = J_1 t^\gamma \quad (12)$$

Thus, the viscoelastic compliance defined by Eq. (4) takes the following form

$$J = J_0 + J_1 t^\gamma, \quad (13)$$

where J_0, J_1 and γ are the material parameters which can be determined from uniaxial creep tension tests. Furthermore, the evolution law for the rate of the damage parameter w is taken from Kachanov [12] in the form

$$\dot{w} = \left[\frac{\langle \sigma - \sigma_{th} \rangle}{C(1-w)} \right]^r, \quad (14)$$

where C and r are the material parameters, while the square brackets are the McAulay brackets, which means that they vanish if the expression in the brackets is less than zero. Accordingly, the bone behaves as a linear viscoelastic material for stress levels below some threshold value of stress ($\sigma < \sigma_{th}$), and it behaves as a viscoelastic damaging material beyond the threshold ($\sigma > \sigma_{th}$). Assuming that initially $w = w_0$ at $t = 0$, and after performing the integration, Eq. (14) takes the following form [10, 11]

$$\frac{1}{1-w} = \frac{1}{1-w_0} \left\{ 1 - \frac{t}{t_c} \right\}^{-\frac{1}{1+r}} \quad (15)$$

In Eq. (15) t_c is the normalizing constant defined as

$$t_c = \frac{(1-w_0)^{1+r}}{1+r} \left[\frac{C}{\langle \sigma - \sigma_{th} \rangle} \right]^r \quad (16)$$

If we, therefore, denote by w_F the value of w corresponding to the failure of the material and the corresponding time to failure by t_F , the Eqs. (15) and (16) yield

$$t_F = \frac{(1-w_0)^{1+r} - (1-w_F)^{1+r}}{1+r} \left[\frac{C}{\langle \sigma - \sigma_{th} \rangle} \right]^r \quad (17)$$

In the case of elasticity coupled with damage, the ratio of the unloading compliance to the initial loading compliance provides a measure of the level of damage. In particular, it is well-known that (e.g. see the Kachanov relation in [12])

$$\frac{1}{1-w_0} = \frac{J_d}{J_0}, \quad (18)$$

where J_d is the unloading "damaged" compliance evaluated during unloading. Here, the "damaged" compliance J_d is normalized with the initial loading compliance J_0 , as given by the ratio J_d/J_0 . Following the established procedures (Smith and Weitsman [17]), it is assumed that below the threshold of stress ($\sigma < \sigma_{th}$) the normalized compliance does not vary with stress and is insensitive to its level. However, beyond the threshold ($\sigma > \sigma_{th}$) the normalized compliance is enhanced linearly by stress, as follows

$$\frac{J_d}{J_0} = K_T(\sigma) = 1 + k_d (\sigma - \sigma_{th}) H(\sigma - \sigma_{th}), \quad (19)$$

where k_d is the material parameter and H is the unit step function. After inserting Eqs. (11), (13), (15), (18) and (19) into Eq. (9), and after performing the integration, the following equation for the total viscoelastic strain coupled with damage is obtained

$$\varepsilon(t) = K_T \left[J_0 \sigma \left(1 - \frac{t}{t_c} \right)^{-\frac{1}{1+r}} + J_1 \sigma t^\gamma \cdot {}_2F_1(1, \alpha, 1 + \gamma, \beta) \right], \quad (20)$$

where ${}_2F_1$ is the hypergeometric function defined as

$${}_2F_1(1, \alpha, 1 + \gamma, \beta) = 1 + \frac{\alpha}{1+\gamma} \beta + \frac{\alpha(\alpha+1)}{(1+\gamma)(2+\gamma)} \beta^2 + \frac{\alpha(\alpha+1)(\alpha+2)}{(1+\gamma)(2+\gamma)(3+\gamma)} \beta^3 + \dots, \quad (21)$$

with the abbreviations

$$\alpha = \frac{1}{1+r} \quad \text{and} \quad \beta = \frac{t}{t_c} \tag{22}$$

If we consider only the first two terms of the equation (21), the relation for the viscoelastic strain coupled with damage may be expressed in the form

$$\begin{aligned} \varepsilon(t) = K_T \sigma \left\{ J_0 \left[1 - \left(\frac{\sigma - \sigma_{th}}{C} \right)^r \frac{t}{\alpha} \right]^{-\alpha} + \right. \\ \left. + J_1 \sigma t^\gamma \left[1 + \left(\frac{\sigma - \sigma_{th}}{C} \right)^r \frac{t}{1+\gamma} \right]^{-\alpha} \right\} \end{aligned} \tag{23}$$

3 Material parameters

For the presented constitutive model, the material parameters obtained experimentally are taken from Parsamian [7] and Melnis et al. [1]. In order to fit the curve with respect to a series of the creep and creep-recovery data points, Eqs (20) and (23) are simplified as follows

$$\varepsilon(t) = \begin{cases} K_T (J_0 \sigma + J_1 \sigma t^\gamma), & \text{for creep } (0 < t < t_0), \\ J_1 \sigma K_T (t^\gamma - (t - t_0)^\gamma), & \text{for recovery } (t > t_0), \end{cases} \tag{24}$$

where t_0 stands for the recovery time, and K_T is the ratio of "damaged" and initial compliance (J_d/J_0)

$$K_T = \begin{cases} 1 & \text{for } \sigma < \sigma_{th}, \\ 1 + k_d (\sigma - \sigma_{th}) & \text{for } \sigma > \sigma_{th}. \end{cases} \tag{25}$$

Here, in obtaining Eq. (24) only the first term of the right-

hand side of Eq. (21) is taken into account.

3.1 Creep material parameters

Parsamian [7] used in his experiments the specimens machined from the right tibia cortical bone from a 54-year old man. Short creep tests were carried out by applying a constant tensile load along the bone longitudinal axis for five loading levels corresponding to a normal stress of 59,66; 61,55; 63,43; 66,97 and 74,73 MPa (specimens are referred to as T12, T11, T7, T10 and T9). As reported in [7], the material parameters r and C were obtained by the curve fitting creep rupture data ($r = 11,265$, $C = 36,617$). On the other hand, the viscoelastic parameters J_0 , J_1 and γ were calculated by using the data from short term creep tests, loaded below the threshold stress levels (prior to the initiation of damage). In this case, the estimated threshold value of stress (σ_{th}) was 75,29 MPa. Fondrk et al. [2] presented a range of human bone constants from 68 to 79 MPa for the threshold stress that agree well with those obtained by Parsamian [7].

The results for the material parameters are summarized in Tab. 1. The average values, given in Tab. 1, are used for the finite element predictions of the model. A graphical representation of the time dependence of the cortical bone stress-strain behaviour is given in Fig. 2.

3.2 Creep-recovery material parameters

In order to model the creep-recovery behaviour of cortical bone, the material parameters are determined by fitting the experimental results obtained by Melnis et al [1]. As described in this paper, the experimental samples were taken from the middle segment of the tibia diaphysis from five males, ranging in age from 30 to 35. The samples were cut along the longitudinal axis of the bone in six cross-sectional zones. Two samples were prepared along the thickness of each zone (outer and inner layer). Thereafter, creep-recovery testing was carried out at six different stress

Table 1 Material parameters obtained experimentally from creep tests [7]

Specimen	σ / MPa	J_0 / MPa ⁻¹	J_1 / MPa ⁻¹ · s ^{-γ}	γ
T7	63,43	37,734	12,482	0,0695
T9	74,73	46,262	4,621	0,0890
T10	66,97	27,432	15,6	0,0550
T11	61,55	41,349	9,998	0,0929
T12	59,66	36,74	10,907	0,0560
average values	-	37,9034	10,7216	0,0724

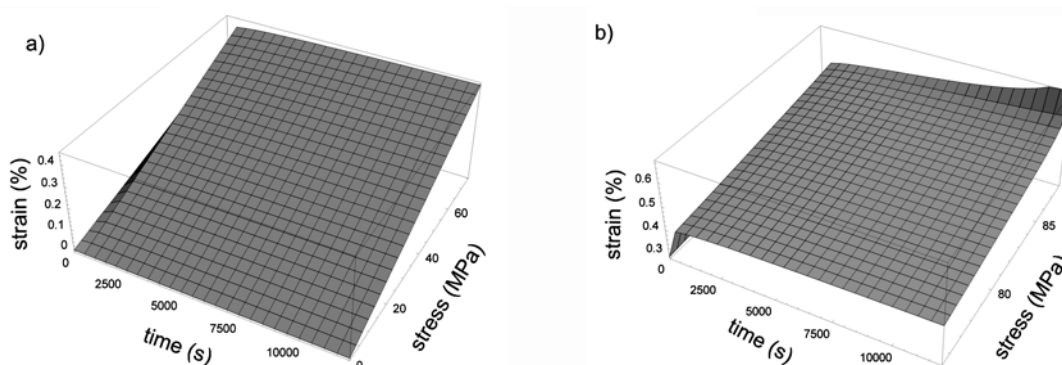


Figure 2 Time-dependence of the stress-strain behaviour of cortical bone below a) and above b) the threshold value of stress ($\sigma_{th} = 75,29$ MPa)

levels between 30 and 105 MPa.

Based on the experimental results, the dependence of the normalized compliance (ratio between the unloading and initial compliances J_d/J_0) with the creep stress of the cortical bone is obtained.

The results shown in Fig. 3 are consistent with Eq. (25) and the assumption that below threshold value of stress the normalized compliance does not vary with stress ($J_d/J_0 = 1$), while above the threshold value of stress a linear correlation between the ratio J_d/J_0 and stress occurs. Here, the filled circles are the experimental data, while the solid line represents a fit of Eq. (19) to these data. The best fits of the data to Eq. (19) gave the following values for the threshold stress and normalizing constant: $\sigma_{th} = 70,5$ MPa, $k_d = 0,002314$ ($R^2 = 0,9989$). The suitability of fitting is judged by the coefficient of determination R^2 [20]. The threshold value of stress, estimated in such a manner, is within the limits presented in the paper [2].

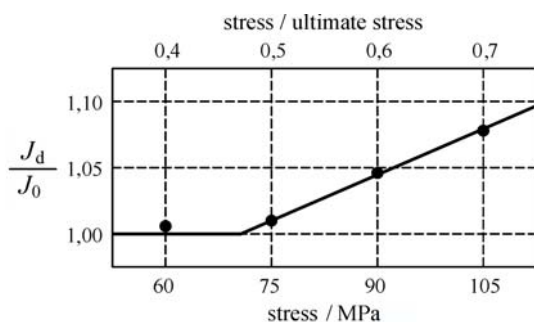


Figure 3 Dependence of the ratio between the unloading and initial compliances J_d/J_0 on the creep stress of cortical bone

Furthermore, in order to determine the viscoelastic parameters J_0, J_1 and γ from the experimental data presented in [1], the procedure proposed by Dasappa et al. [21] is used in this study. These parameters are estimated using the creep/creep-recovery tests data performed at various stress levels. Firstly, the permanent (viscoplastic) strain $\epsilon_{vp}(t_r)$ (see Fig. 1) is obtained as the total unrecovered strain after very long recovery periods. The recovery period in the experimental data by Melnis et al. [1] is 5 times longer than the creep period. Viscoelastic strain is then obtained by subtracting the permanent strain $\epsilon_{vp}(6t_0)$ from the total strain or the creep-recovery data ($\epsilon_r(t) - \epsilon_{vp}(6t_0)$) (Fig. 4). After that, the viscoelastic parameters are obtained. In [17] a similar

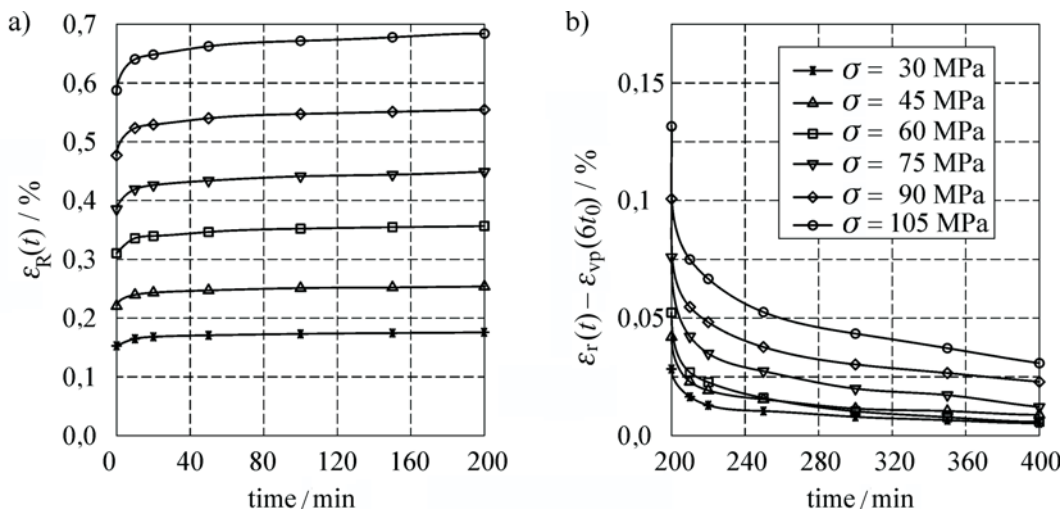


Figure 4 Creep/creep-recovery curves for viscoelastic parameters determination

procedure is proposed where the viscoelastic parameters J_1 and γ are determined from the creep-recovery curve (Fig. 4b), and J_0 from the creep curve (Fig. 4a) under a small loading where the plastic strain does not exist. The material parameters determined by fitting the experimental results of the creep/creep-recovery tests [1] presented in Fig. 4 are given in Tab. 2. Using these parameters and Eqs. (24) and (25), a graphical representation of the creep-recovery strain as a function of time and stress for human cortical bone is obtained as shown in Fig. 5.

4 Numerical formulation

In this section, the time discretisation and computational integration procedures for the presented viscoelastic/damage model are given. An algorithm for integrating the similar one-dimensional constitutive model has recently been proposed by Lovrenić-Jugović et al. in [8, 9]. In the present study, this computational algorithm is modified for a better description of damage accumulation in the cortical bone tissue subjected to a creep-recovery loading. In order to implement the proposed viscoelastic-damage model into the finite element algorithm, the constitutive equations are transformed into an incremental form by using finite differences. The updated values of the state variables, $\sigma(t_n + \Delta t)$ and $\epsilon(t_n + \Delta t)$, at the end of the time step $(t_n, t_n + \Delta t)$ have to be found for a given value of the incremental strain $\Delta \epsilon(t_n)$ at time t_n . The constitutive equations are transformed into an incremental form by using the following integration operator

$$f_{t_n + \Delta t} = f_{t_n} + \Delta f, \tag{26}$$

where f is some function, f_{t_n} is its value at the beginning of the increment, Δf is the change in the function over the increment, and Δt is the time increment.

4.1 Viscoelasticity

For the stress levels below the threshold value of stress ($\sigma < \sigma_{th}$) (Parsamian [7]: $\sigma_{th} = 75,29$ MPa, Melnis et al. [1]: $\sigma_{th} = 70,5$ MPa), Eq. (24) may be expressed by the following incremental relation

Table 2 Material parameters determined by fitting the experimental results of creep/creep-recovery tests [1] presented in Fig. 4

Viscoelastic parameters	Value	Standard Error	Units	R^2
J_1	$8,61449 \times 10^{-7}$	$1,51269 \times 10^{-7}$	$\text{MPa}^{-1} \cdot \text{s}^{-\gamma}$	0,94219
γ	0,27124	0,01606	-	
J_0	$5,2217 \times 10^{-5}$	$4,17008 \times 10^{-7}$	MPa^{-1}	0,98651

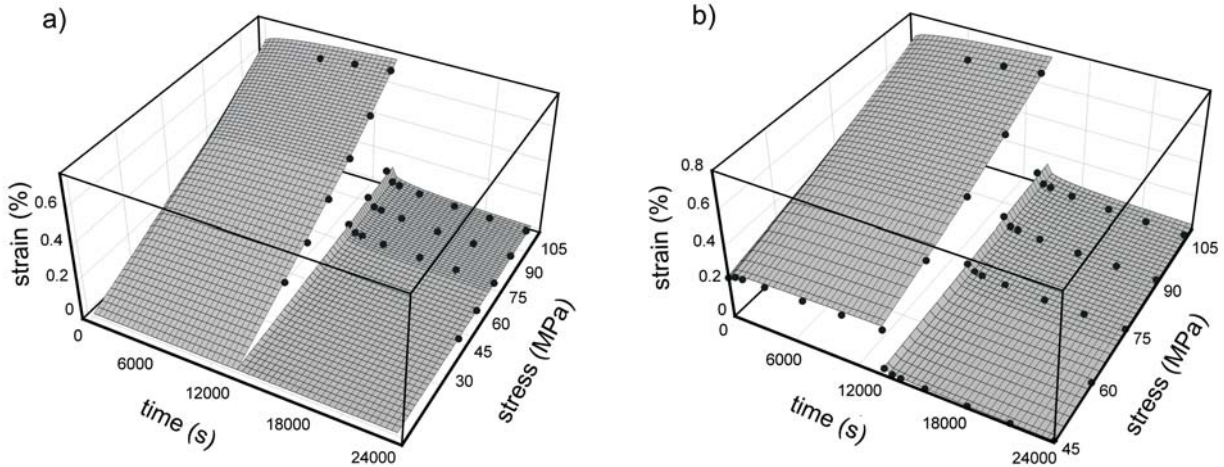


Figure 5 Time-dependence of the stress-strain behaviour of cortical bone. The filled circles are the experimental data from [1]

$$\Delta\sigma = E_{t_n+\Delta t} \cdot (\varepsilon + \Delta\varepsilon) - \sigma, \quad \sigma < \sigma_{th}, \quad (27)$$

where

$$E_{t_n+\Delta t} = \begin{cases} \frac{1}{J_0 + J_1 (t + \Delta t)^\gamma}, & (0 < t < t_0), \\ \frac{1}{J_1 [(t + \Delta t)^\gamma - (t + \Delta t - t_0)^\gamma]}, & (t > t_0). \end{cases} \quad (28)$$

In order to preserve the numerical efficiency of the global iteration strategy, the tangent stiffness matrix or the Jacobian matrix is derived and applied thereby. This matrix is obtained using the tangent modulus relating the infinitesimal increase in the stress to the infinitesimal increase in the strain. After the differentiation of Eq. (27), the tangent stiffness is obtained as

$$\frac{\partial \Delta\sigma}{\partial \Delta\varepsilon} = E_{t_n+\Delta t}, \quad \sigma < \sigma_{th}, \quad (29)$$

where $E_{t_n+\Delta t}$ follows from Eq. (28).

4.2 Viscoelasticity coupled with damage

For stress levels above the threshold value of stress ($\sigma > \sigma_{th}$), after some suitable formula manipulations Eq. (24) may be rewritten in the following nonlinear form

$$F_{t_n+\Delta t} = E_{t_n+\Delta t} (\varepsilon + \Delta\varepsilon) - (\sigma + \Delta\sigma) = 0, \quad \sigma > \sigma_{th}, \quad (30)$$

where

$$E_{t_n+\Delta t} = \begin{cases} \frac{1}{A [J_0 + J_1 (t + \Delta t)^\gamma]}, & (0 < t < t_0), \\ \frac{1}{J_1 A [(t + \Delta t)^\gamma - (t + \Delta t - t_0)^\gamma]}, & (t > t_0), \end{cases} \quad (31)$$

with the abbreviation

$$A = 1 + k_d (\sigma + \Delta\sigma - \sigma_{th}). \quad (32)$$

The above nonlinear Eq. (31) is solved by the Newton-Raphson iterative method, and, thus

$$\Delta\sigma^{(i+1)} = \Delta\sigma^{(i)} - \frac{F_{t_n+\Delta t}^{(i)}}{\left(\frac{dF_{t_n+\Delta t}}{d\Delta\sigma}\right)^{(i)}}, \quad (33)$$

where $(i+1)$ abbreviates the current iteration step, and $(dF_{t_n+\Delta t}/d\Delta\sigma)^{(i+1)}$ is calculated analytically by

$$\left(\frac{dF_{t_n+\Delta t}}{d\Delta\sigma}\right)^{(i)} = -\frac{E_{t_n+\Delta t} \cdot (\varepsilon + \Delta\varepsilon) \cdot k_d}{1 + k_d (\sigma + \Delta\sigma - \sigma_{th})} - 1. \quad (34)$$

Using Eq. (30), the explicit expression for the tangent stiffness is obtained

$$\frac{\partial \Delta\sigma}{\partial \Delta\varepsilon} = \frac{E_{t_n+\Delta t}}{1 + \frac{(\varepsilon + \Delta\varepsilon) \cdot E_{t_n+\Delta t} \cdot k_d}{1 + k_d (\sigma + \Delta\sigma - \sigma_{th})}}, \quad \sigma > \sigma_{th}. \quad (35)$$

In Eqs. (34) and (35) $E_{t_n+\Delta t}$ follows from Eq. (31).

For more accurate prediction of viscoelastic strain coupled with damage, instead of Eq. (24), Eq. (23) can be

used. In this case, the following incremental relations can be obtained from Eq. (23):

a) for creep ($0 < t < t_0$):

$$F_{t_n+\Delta t} = -\varepsilon - \Delta\varepsilon + A(\sigma + \Delta\sigma) \left\{ J_0 \left[1 - B^r \frac{t+\Delta t}{\alpha} \right]^{-\alpha} + J_1 (t + \Delta t)^\gamma \left[1 + B^r \frac{t+\Delta t}{1+\gamma} \right] \right\}, \quad (36)$$

$$\begin{aligned} \left(\frac{dF_{t_n+\Delta t}}{d\Delta\sigma} \right)^{(i)} &= D \left[J_0 \left(1 - B^r \frac{t+\Delta t}{\alpha} \right)^{-\alpha} + J_1 (t + \Delta t)^\gamma \left(1 + B^r \frac{t+\Delta t}{1+\gamma} \right) \right] + \\ &+ A(\sigma + \Delta\sigma) \frac{r}{C} B^{r-1} (t + \Delta t) \cdot \\ &\cdot \left\{ J_0 \left[1 - B^r \frac{t+\Delta t}{\alpha} \right]^{-\alpha-1} + J_1 (t + \Delta t)^\gamma \frac{1}{1+\gamma} \right\}, \end{aligned} \quad (37)$$

$$\frac{\partial \Delta\sigma}{\partial \Delta\varepsilon} = 1 / \left(\frac{dF_{t_n+\Delta t}}{d\Delta\sigma} \right), \quad (38)$$

b) for recovery ($t > t_0$):

$$F_{t_n+\Delta t} = -\varepsilon - \Delta\varepsilon + A(\sigma + \Delta\sigma) \cdot J_1 \left[(t + \Delta t)^\gamma - (t + \Delta t - t_0)^\gamma \right] \cdot \left[1 + B^r \frac{t+\Delta t}{1+\gamma} \right], \quad (39)$$

$$\begin{aligned} \left(\frac{dF_{t_n+\Delta t}}{d\Delta\sigma} \right)^{(i)} &= DJ_1 \left[(t + \Delta t)^\gamma - (t + \Delta t - t_0)^\gamma \right] \cdot \\ &\cdot \left[1 + B^r \frac{t+\Delta t}{1+\gamma} \right] + A(\sigma + \Delta\sigma) J_1 \cdot \\ &\cdot \left[(t + \Delta t)^\gamma - (t + \Delta t - t_0)^\gamma \right] \cdot \\ &\cdot \frac{1}{1+\gamma} \frac{r}{C} B^{r-1} (t + \Delta t), \end{aligned} \quad (40)$$

$$\frac{\partial \Delta\sigma}{\partial \Delta\varepsilon} = 1 / \left(\frac{dF_{t_n+\Delta t}}{d\Delta\sigma} \right). \quad (41)$$

In Eqs. (36), (37), (39) and (40) the following abbreviations are introduced

$$B = \frac{\sigma + \Delta\sigma - \sigma_{th}}{C}, \quad (42)$$

$$D = \left[1 + k_d (2\sigma + 2\Delta\sigma - \sigma_{th}) \right]. \quad (43)$$

After determining the stress increment $\Delta\sigma$, the updated value of the stress tensor, as well as all internal variables, can be calculated. The derived integration algorithm and the corresponding tangent stiffness have been implemented at the material point level of the three-dimensional solid continuum finite elements in the software ABAQUS/Standard [14] by using the user-defined material subroutine UMAT.

5 Numerical results

In order to validate the numerical algorithm proposed, the creep and recovery simulation results are compared with the experimental data. The FE model considered here is, simply, a three-dimensional single finite element (linear brick C3D8 element), used to obtain the response due to the uniaxial creep-recovery loading. A tension load is first applied to the FE model using an elastic calculation at time $t = 0$. After this instantaneous loading, the load is kept constant for some period of time, and subsequent time-dependent creep analyses are performed.

After the creep period, the applied load is removed and held at zero during the recovery period (see Fig. 1).

5.1 Creep tests

The FE model with the calibrated material parameters, shown in Tab. 1, is used to analyze the response of bone to creep loading. Fig. 6 shows a comparison between the experimental data and the predictions at different combinations of stress levels. Furthermore, good agreement between the experimental measurements and present algorithm is observed in Fig. 6. The predictions deviate from the experimental results only for the cases in which the averaged values of the material parameters are taken from Tab. 1. Additionally, it is found that if we approximate the hypergeometric function by using only the first term or the first two terms in the series (the right-hand side of Eq. (21)), similar results are obtained.

5.2 Creep-recovery tests

Moreover, the derived numerical algorithm with the material parameters calibrated by fitting the experimental results obtained by Melnis et al. [1] (see Tab. 2), is used to analyze the response of bone to creep-recovery tests. A comparison of strain versus time between the solutions obtained in the present paper and the published experimental [1] and numerical [15] solutions for creep and recovery tests at three different stress levels is shown in Fig. 7. Again, good agreement is obtained between the experiments and the numerical model. Only a slight difference occurs in the recovery period in Fig. 7c), where the applied stress during the creep period was 90 MPa. The reason for this is that our model neglects the effect of viscoplastic deformation which increases with increasing the applied stress level.

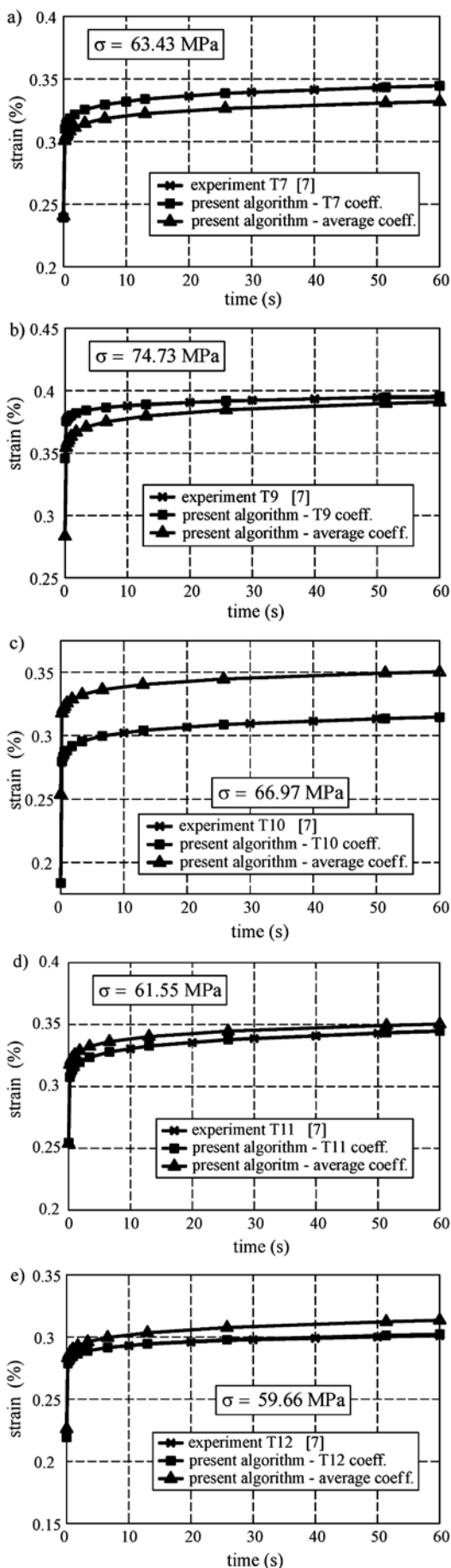


Figure 6 Comparison of strain versus time between the present study and the published experimental measurements by Parsamian [7] for: a) 63,43 MPa, b) 74,73 MPa, c) 66,97 MPa, d) 61,55 MPa and e) 59,66 MPa.

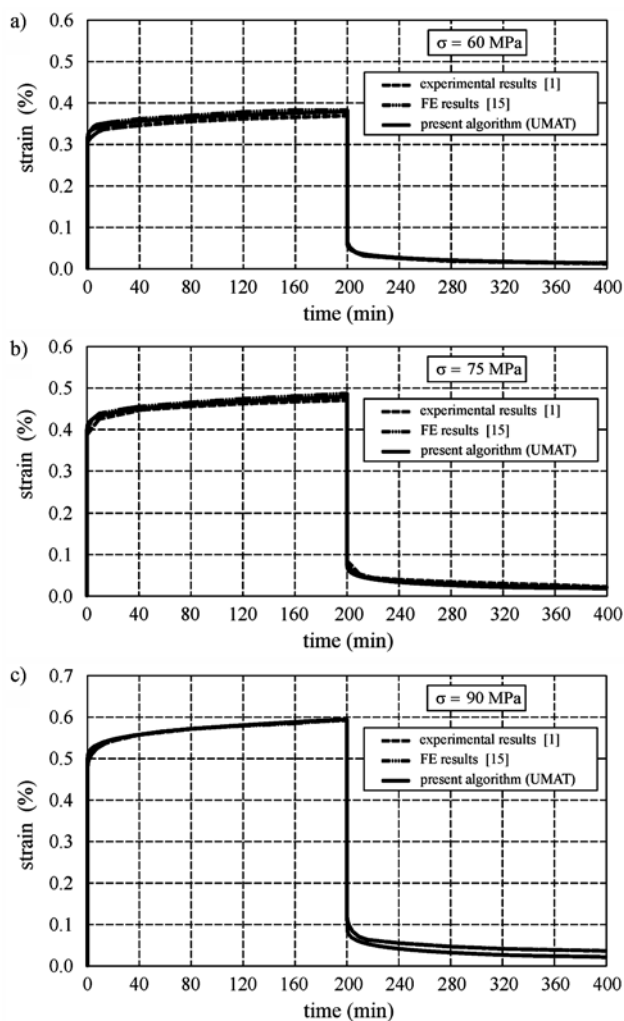


Figure 7 Comparison of strain versus time between the present study and the published experimental [1] and numerical [15] solutions at: a) 60 MPa, b) 75 MPa, c) 90 MPa

6 Conclusion

A three-dimensional constitutive model for the human cortical bone tissue to predict the experimental viscoelastic/damage behaviour in creep-recovery tests is presented. For the proposed constitutive model, the material parameters are determined by fitting the experimental results of the creep-recovery tests carried out by Parsamian [7] and Melnis et al [1]. Small strains are assumed and, for simplification purposes, the influence of permanent strains is neglected. A computational algorithm for the integration of the proposed constitutive model is derived and implemented in an Abaqus UMAT subroutine. The accuracy of the computational procedure is verified by comparing the model predictions with the published experimental data and numerical solutions. Thereby, the creep and creep-recovery deformation processes in cortical bone at different loading levels are considered. The computational algorithm shows an excellent capability to describe the tensile behaviour of cortical bone for the specific mechanical condition analysed.

The present analysis considers only the uniaxial creep-recovery test of human bone. Therefore, to fully validate the presented constitutive model, it is necessary to analyze additional tests. Moreover, future study will focus on coupling the presented viscoelastic/damage model with a viscoplastic framework [22, 23] and extending this model to

more complex orthotropic material behaviour. Hence, more extensive and accurate experimental data are required to determine the material parameters and fully validate the computational model, which is the scope of the current study by the authors.

Acknowledgments

This study is supported by the Ministry of Science, Education and Sports of the Republic of Croatia within the framework of the Research Project No. 120- 1201910-1906.

7

References

- [1] Melnis, A. E.; Knets, I. V.; Moorlat, P. A. Deformation behavior of human compact bone tissue upon creep under tensile testing. // *Mechanics of Composite Materials*. 15, (1980), pp. 574-579.
- [2] Fondrk, M.; Bahniuk, E.; Davy, D. T.; Michaels, C. Some viscoplastic characteristics of bovine and human cortical bone. // *Journal of Biomechanics*. 21, 8(1988), pp. 623-630.
- [3] Ott, I.; Kienzler R.; Schroeder, R. Aging in the cortical bone: a constitutive law and its application. // *Archive of Applied Mechanics*. 80, (2010), pp. 527-541.
- [4] Luo, Q.; Leng, H.; Acunae, R.; Dong, X. N.; Rong, Q.; Wang, X. Constitutive relationship of tissue behavior with damage accumulation of human cortical bone. // *Journal of Biomechanics*, 43, (2010), pp. 2356-2361.
- [5] Garcia, D.; Zysset, P. K.; Charlebois, M.; Curnier, A. A three-dimensional elastic plastic damage constitutive law for bone tissue. // *Biomechanics and Modeling in Mechanobiology*. 8, 2(2008), pp. 149-165.
- [6] Garcia, D.; Zysset, P. K.; Charlebois, M.; Curnier, A. A 1-D elastic plastic damage constitutive law for bone tissue. // *Archive of Applied Mechanics*. 80, (2010), pp 543-555.
- [7] Parsamian, G. P. Damage mechanics of human cortical bone. / PhD Thesis, West Virginia University (2001).
- [8] Lovrenić-Jugović, M.; Tonković, Z.; Skozrit, I. Numerical modelling of viscoelastic/damage behaviour of cortical bone. // *Key Engineering Materials*. 417-418, (2010), pp. 273-276.
- [9] Lovrenić-Jugović, M.; Tonković, Z.; Skozrit, I.; Pustačić, D. On numerical modelling of nonlinear behaviour of cortical bone. // 6th International Congress of Croatian Society of Mechanics / uredili Smojver, I.; Sorić, J. Dubrovnik, Croatia, 2009, CD-ROM edition.
- [10] Abdel-Tawab, K.; Weitsman, Y. J. A strain-based formulation for the coupled viscoelastic/damage behavior. // Contract technical report, The University of Tennessee, 1997.
- [11] Abdel-Tawab, K.; Weitsman, Y. J. A coupled viscoelasticity/damage model with application to swirl-mat composites. // *International Journal of Damage Mechanics*. 7, (1997), pp. 351-380.
- [12] Kachanov, L. M. Introduction to Continuum Damage Mechanics. Martinus Nijhoff, Dordrecht, 1986.
- [13] Lemaitre, J. A Course on Damage Mechanics. Springer-Verlag, New York, 1992.
- [14] ABAQUS/Standard, User's guide and theoretical manual, Version 6.10.1, Dassault Systemes, 2010.
- [15] Natali, A. N.; Meroi, E. A. A review of the biomechanical properties of bone as a material. // *Journal of Biomedical Engineering*. 11, (1989), pp. 266-276.
- [16] Lovrenić-Jugović, M.; Tonković, Z.; Skozrit, I. Modelling of Nonlinear Creep and Recovery Behaviour of Cortical Bone. // *Key Engineering Materials*. 488-489, (2011), pp. 186-189.
- [17] Smith, L. V.; Weitsman, Y. J. The visco-damage mechanical response of swirl-mat composites. // *International Journal of Fracture*. 97, (1999), pp. 301-319.
- [18] Schapery, R. A. Nonlinear viscoelastic solids. // *International Journal of Solids and Structure*. 37, (2000), pp. 359-366.
- [19] Pipkin, A. C. Lectures on viscoelasticity theory, 2nd Ed., Applied Mathematical Sciences, Vol. 7, Springer-Verlag, New York, 1986.
- [20] Iyo, T.; Maki, Y.; Sasaki, N.; Nakata, M. Anisotropic viscoelastic properties of cortical bone. // *Journal of Biomechanics*. 37, (2004), pp. 1433-1437.
- [21] Dasappa, P.; Lee-Sullivan, P.; Xiao, X. Development of viscoplastic strains during creep in continuous fibre GMT composites. // *Composites: Part B*. 41, (2010), pp. 48-57.
- [22] Sorić, J.; Tonković, Z.; Krätzig, W. B. A New Formulation of Numerical Algorithms for Modeling of Elastoplastic Cyclic Response of Shell-Like Structures. // *Computers & Structures*. 78, 1-3(2000), pp. 161-168.
- [23] Tonković, Z.; Sorić, J.; Skozrit, I. On Numerical Modeling of Cyclic Elastoplastic Response of Shell Structures. // *Computer Modeling in Engineering & Sciences*. 26, 2(2008), pp. 75-90.

Authors' addresses

Martina Lovrenić-Jugović

University of Zagreb
Faculty of Mechanical Engineering and Naval Architecture
Institute of Applied Mechanics
Laboratory of Numerical Mechanics
Ivana Lučića 5
10000 Zagreb, Croatia
e-mail: martina.lovrenic@fsb.hr

Prof. dr. sc. Zdenko Tonković

University of Zagreb
Faculty of Mechanical Engineering and Naval Architecture
Institute of Applied Mechanics
Laboratory of Numerical Mechanics
Ivana Lučića 5
10000 Zagreb, Croatia
e-mail: zdenko.tonkovic@fsb.hr

Dr. sc. Ivica Skozrit

University of Zagreb
Faculty of Mechanical Engineering and Naval Architecture
Institute of Applied Mechanics
Laboratory of Numerical Mechanics
Ivana Lučića 5
10000 Zagreb, Croatia
e-mail: ivica.skozrit@fsb.hr